

Characterizing ecohydrological and biogeochemical connectivity across multiple scales: a new conceptual framework

Lixin Wang,^{1*} Chris Zou,² Frances O'Donnell,¹ Stephen Good,¹ Trenton Franz,¹ Gretchen R. Miller,³ Kelly K. Caylor,¹ Jessica M. Cable⁴ and Barbara Bond⁵

¹ Department of Civil and Environmental Engineering, Princeton University, Princeton, NJ 08544, USA

² Department of Natural Resource Ecology and Management, Oklahoma State University, Stillwater, OK, USA

³ Department of Civil Engineering, Texas A&M University, College Station, TX, USA

⁴ International Arctic Research Center, University of Alaska, Fairbanks, AK, USA

⁵ Department of Forest Ecosystems and Society, Oregon State University, Corvallis, OR 97331, USA

ABSTRACT

The connectivity of ecohydrological and biogeochemical processes across time and space is a critical determinant of ecosystem structure and function. However, characterizing cross-scale connectivity is a challenge due to the lack of theories and modelling approaches that are applicable at multiple scales and due to our rudimentary understanding of the magnitude and dynamics of such connectivity. In this article, we present a conceptual framework for upscaling quantitative models of ecohydrological and biogeochemical processes using electrical circuit analogies and the Thévenin's theorem. Any process with a feasible linear electrical circuit analogy can be represented in larger scale models as a simplified Thévenin equivalent. The Thévenin equivalent behaves identically to the original circuit, so the mechanistic features of the model are maintained at larger scales. We present three case applications: water transport, carbon transport, and nitrogen transport. These examples show that Thévenin's theorem could be a useful tool for upscaling models of interconnected ecohydrological and biogeochemical systems. It is also possible to investigate how disruptions in micro-scale connectivity can affect macro-scale processes. The utility of the Thévenin's theorem in environmental sciences is somewhat limited, because not all processes can be represented as linear electrical circuits. However, where it is applicable, it provides an inherently scalable and quantitative framework for describing ecohydrological connectivity. Copyright © 2010 John Wiley & Sons, Ltd.

KEY WORDS carbon cycling; electrical circuit; nitrogen cycling; nutrient cycling; scaling; soil-plant-atmosphere continuum; Thévenin's theorem; watershed

Received 12 August 2010; Accepted 17 November 2010

INTRODUCTION

Connectivity has different definitions in various disciplines. For example, in population studies, connectivity is the degree to which the landscape facilitates or impedes movement among resource patches (Taylor *et al.*, 1993; Tischendorf and Fahrig, 2000); in network communication, connectivity refers to the status that network remains connected so that information collected by sensor nodes can be relayed back to data sinks or controllers (Zhang and Hou, 2005). Recently, the connectivity concept has been applied to various physical processes within and among ecosystems to better understand system dynamics at large scales (Peters *et al.*, 2006), although it is not accurately defined in ecosystem studies. The working definition of connectivity in this article is the connections in ecological or hydrological processes that appear within or among different spatial scales.

The abiotic media that connect environmental systems include carbon, water, nutrients, energy, and momentum,

as well as the interactions among them (Austin *et al.*, 2004; Wang *et al.*, 2009). One of the major advantages of studying connectivity in physical processes is to understand the cross-scale interactions. For example, how do variations of ribulose-1,5-bisphosphate carboxylase-oxygenase (RuBisCo) function in C₃ and C₄ plants affect landscape scale CO₂ fluxes. This knowledge will significantly improve our system predictions at larger scale based on information from smaller scales (Peters *et al.*, 2004). However, quantifying cross-scale connectivity is still a major challenge due largely to the lack of theories and modelling approaches that are applicable at multiple scales. Analogical models offer a potential approach for quantifying cross-scale connectivity, which simulate the behaviours of complex physical systems using laws and theorems known to control component processes. Such models have been successfully applied to simulate flows of matter and energy in environmental systems. A well-known example of analogical modelling in environmental science is the parallel between Ohm's law for electric current flow (Honert, 1948) and Darcy's law (phenomenologically derived constitutive equation that describes the

* Correspondence to: Lixin Wang, Department of Civil and Environmental Engineering, Princeton University, Princeton, NJ 08544, USA.
E-mail: lixinw@princeton.edu

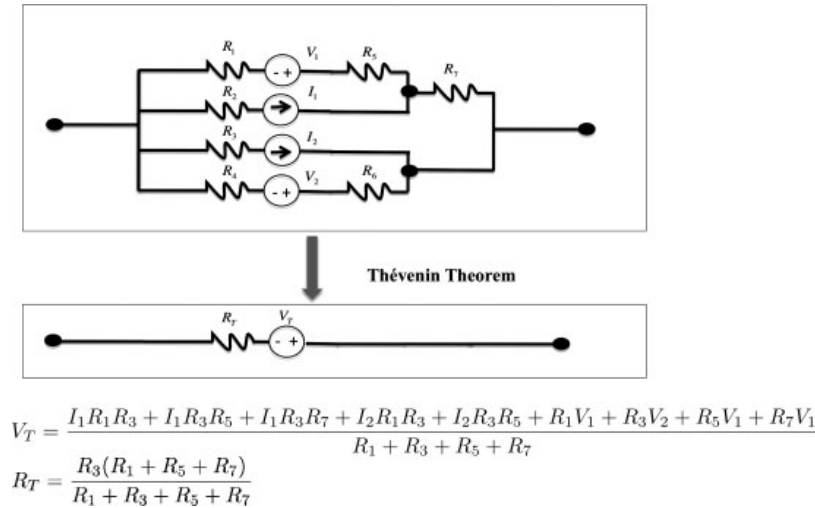


Figure 1. An example of application of Thévenin's theorem to simplify electrical circuit. R_1 to R_7 are resistors, V_1 and V_2 are voltage source, and I_1 and I_2 are current source. R_T and V_T are the corresponding Thévenin equivalents solved based on the Thévenin's theorem.

flow of a fluid through a porous medium) for groundwater flow (Dingman, 2008). The description of biophysical processes with electrical circuit theory has many other applications in the environmental sciences, including the modelling of evapotranspiration as the resistance terms in the Penman–Monteith equation (Jones, 1992).

In this article, we formulate analogical models that are able to connect biophysical processes acting at different scales through a consistent framework. The paradigm may provide insight into landscape connectivity as well as interactions between micro- and macro-scale ecohydrological and biogeochemical processes. Specifically, our objective is to evaluate the applicability of using electrical circuit analogies and the Thévenin's theorem to upscale connectivity in a quantitative manner. Although the theorem has been applied in electrical circuit theory for over a century, its application in the environmental sciences is relatively new (Campbell, 2003).

The Thévenin's theorem is used to simplify electrical circuits. It states that any linear combination of voltage sources, current sources, and resistances can be equivalently represented by one resistor in series with one voltage source (Dorf and Svoboda, 2006). Therefore, ecosystem processes with linear electrical analogies could be represented by their Thévenin equivalents in larger scale models. This allows detailed interactions at a small scale to be represented simply when scaling up. The representation of hydrological systems with electrical analogies has a long history in the environmental sciences (e.g. resistance terms in Penman–Monteith equation). The Thévenin's theorem would provide new opportunities for using electrical analogies to systematically describe and quantify connectivity should this framework prove to be practically achievable over a wide range of processes.

Thévenin's theorem: concept and principles

A key set of theorems from electrical circuit theory are the Thévenin's and Norton's theorems that allow for

linear circuits of resistors, current sources, and voltage sources of any size and configuration with two terminals to be represented by a single resistor and a single voltage source in series (Thévenin's theorem) or a single resistor and a single current source in parallel (Norton's theorem) (Boylestad, 1982). The simplified 'equivalent circuit' behaves exactly as the larger circuit from the voltage point of the connecting terminals (Dorf and Svoboda, 2006) (Figure 1). Campbell (2003) applied Thévenin's theorem to an electrical circuit model of sensible and latent heat flux from plant canopies, representing the flux of enthalpy and isothermal latent heat with a single resistor and voltage source for each component flux. In this work, we demonstrate the broad potential use of the Thévenin's theorem to represent different ecological/hydrological processes (e.g. root water uptake and carbon fixation at cell level) at small scales with a simplified equivalent circuit, then subsequently use these equivalent circuits as building blocks of analogy networks representing processes at larger scales (e.g. watershed scale leaching). In this fashion, we are able to maintain representation of process at the micro-scale when modelling at the macro-scale.

Application of the Thévenin's theorem involves two steps. First, the two terminals are connected with an open circuit, and the voltage across the open connection is calculated as the Thévenin equivalent voltage (V_{th}). Second, any independent sources are deactivated and the Thévenin resistance (R_{th}) is found through circuit resistance reduction. The Thévenin equivalent circuit is then made of one ideal voltage source (V_{th}) in series with a single resistor (R_{th}). More complicated cases involving independent and dependent sources may also be resolved into a Thévenin equivalent circuit, and the reader is directed to introductory circuit analysis texts for further information (Boylestad, 1982; Dorf and Svoboda, 2006). In the event that the particular configuration of the circuit in question is not known, the Thévenin equivalent may

Table I. Electrical analogies to ecohydrological and biogeochemical parameters and the corresponding units.

	Water	Carbon	Nitrogen
Voltage (V)	Water potential difference, Ψ (Pa)	Concentration difference of carbon compounds (mol/m^3)	Concentration difference of nitrogen compounds (mol/m^3)
Current (I)	Mass flow through system, Q ($\text{kg}/\text{m}^2/\text{s}$)	Carbon flux density ($\text{mol}/\text{m}^2/\text{s}$)	Nitrogen flux density ($\text{mol}/\text{m}^2/\text{s}$)
Resistance (R)	Resistance to water movement through soil pores, plant xylem, and the leaf–atmosphere interface ($\text{kg}/\text{m}^2/\text{Pa}$)	Impedance to carbon flow of a link in the system (s/m)	Impedance to nitrogen flow of a link in the system (s/m)

still be determined. For example, in the laboratory, a variable resistor and voltmeter can be connected to the terminals of the circuit in question, and a series of voltage measurements are then taken for different resistor values. Voltage is then plotted as a function of resistance, and a line fit to the data. The slope of this line is then V_{th} and the intercept is R_{th} (Dorf and Svoboda, 2006).

In the following sections, we evaluate the applicability of the Thévenin's theorem to three processes across multiple scales: water transport, carbon transport, and nitrogen transport.

Case applications

Case I—water transport in plant, hillslope and watershed. Water transport processes define critical ecohydrological interactions and connections. Substantial progress has been made in terms of understanding how water flux and transport affects ecological processes and vegetation dynamics and vice versa. The integrated understanding of ecohydrological interactions and connections at multiple scales will help solve issues related to land use, land cover, and climate changes, which remain a challenging task. Such a challenge is neither trivial nor unique to ecohydrology. Transport of water follows physical rules although its description is typically empirical. Complicated interactions and connectivity between ecological and hydrological processes at multiple scales may be described and quantified using physical principles. In this section, we first illustrate the ecohydrological interactions at the plant, hillslope, and watershed levels using electrical circuit analogy based on our current understanding of water transport and then connect these processes at different levels through the Thévenin's theorem. In the theorem, the analogy of current is represented by water flux, which is driven by the gradient of water potential and regulated by biotic attributes and processes (such as vegetation functional type and leaf area index) or by abiotic processes (such as topography, flow path, and atmospheric condition). In this system, we can say $I = V/R$ by Ohm's law, which leads to the following analogies (Table I):

- Voltage (V) is a change in potential energy, represented here by the water potential difference (Ψ), in units of pressure (Pa).

- Resistance (R) is the degree to which an object opposes flow through itself; represented here as the resistance to water movement through soil pores, plant xylem, and the leaf–atmosphere interface. It is in units of $\text{kg}/\text{m}^2/\text{s}/\text{Pa}$, as shown in Dewar (2002).
- Current (I) is the flow of mass through a system, represented as water flux (q) per unit area per time, in units of mass per unit area per time ($\text{kg}/\text{m}^2/\text{s}$).

This exercise will not only provide an example of possibly using the Thévenin's theorem to quantify connectivity across scales but also will illustrate the way of how water cycling connects at each scale using electrical circuit analogy.

Plant and soil level

Water transport in plants has been widely investigated in ecophysiology (Philip, 1966; Kramer, 1974; Tyree and Ewers, 1991; Kramer and Boyer, 1995) and is well summarized by the soil–plant–atmospheric continuum (SPAC) concept (Jarvis *et al.*, 1981; Tuzet *et al.*, 2003). The SPAC is still one of the best frameworks to describe the water transport pathway and connectivity between the soil and atmosphere, and the electrical analogy diagram of SPAC can be described in Figure 2.

As shown in Figure 2(a), with respect to the plant resistor, all water flow is driven by potential gradients between the soil and atmosphere and the atmosphere basically serves as a ground. Soil moisture [$I_{\text{soil_moisture}}(P, T, \text{Soil, Vege})$] is a current source, which is a function of precipitation after accounting for interception losses by canopy and litter, temperature, soil properties, and vegetation properties. Soil moisture here is assumed to be a steady-state variable at small time scale to meet the circuit analogy requirement. The soil water potential, $\Psi_{\text{soil}}(\theta)$, is a function of volumetric water content ($\text{m}^3 \text{m}^{-3}$). Volumetric water content and water potential (pressure) can be related through the soil water retention curves for different soil texture classes (Clapp and Hornberger, 1978; Cosby *et al.*, 1984) or using databases of pedotransfer functions like Rosetta (Schaap *et al.*, 2001). The root potential in the soil, $\Psi_{\text{root}}(\rho, \theta, C_{\text{ions}})$, is a function of root density, root water content, and ion concentration (Fitter and Hay, 1987). The resistance to root water flow is represented by R_{root} (s/m). Next, water

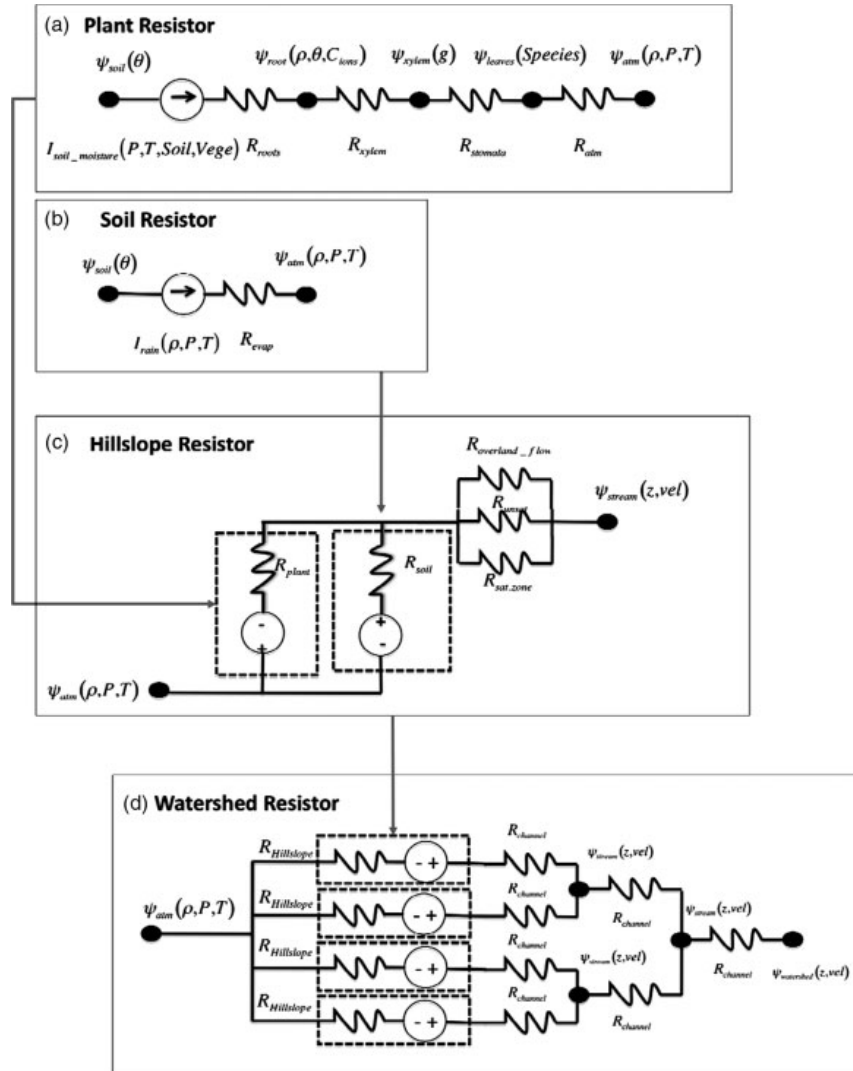


Figure 2. Diagram of electric circuit analogy for water movement at different scales. For plant resistor, $\Psi_{\text{soil}}(\theta)$ is the soil water potential; $I_{\text{soil_moisture}}(P, T, \text{Soil}, \text{Vege})$ is the current source from soil moisture; $\Psi_{\text{root}}(\rho, \theta, C_{\text{ions}})$ is the root potential in the soil; $\Psi_{\text{xylem}}(g, \text{species})$ is the xylem water potential; $\Psi_{\text{leaves}}(\text{species})$ is the leaf water potential; R_{stomata} is the stomata resistance; $\Psi_{\text{atm}}(\rho, e, T)$ is the atmospheric potential; for soil resistor, $\Psi_{\text{soil}}(\theta)$ is the soil water potential; R_{evap} is the resistance of flows from evaporation, including water loss from interception by the canopy, litter, and soil evaporation from the surface; $I_{\text{rain}}(\rho, P, T)$ is current source of water from rainfall; $\Psi_{\text{atm}}(\rho, e, T)$ is the atmospheric potential; for hillslope resistor, R_{plant} (dashed box) and R_{soil} (dashed box) are the Thévenin equivalents of plants and soil; $R_{\text{overland_flow}}$ is the resistances of overland surface flow; R_{unsat} is the resistance of flow due to the shallow unsaturated subsurface zone; R_{satzone} is the resistance of flow from the saturated subsurface; $\Psi_{\text{stream}}(z, \text{vel})$ is the stream channel water potential. For watershed resistor, $R_{\text{hillslope}}$ (dashed boxes) is the Thévenin equivalent of hillslope; $\Psi_{\text{stream}}(z, \text{vel})$ is the stream channel water potential which is a function of the elevation and velocity of the stream; R_{channel} is the resistance of flow due to channel characteristics, such as length and travel time; $\Psi_{\text{watershed}}(z, \text{vel})$ is the watershed potential.

flows through the xylem where the xylem water potential, $\Psi_{\text{xylem}}(g, \text{species})$, is primarily determined by height along the tree stem and is regulated by the gravitational potential, g (m s^{-2}), and frictional resistance along the stem. The resistance to water flow through the xylem vessels is R_{xylem} , which is often represented by xylem conductance $C_{\text{xylem}} = 1/R_{\text{xylem}}$. The leaf water potential, $\Psi_{\text{leaves}}(\text{species})$, is a function of leaf water content and concentration of ions in leaves. The Penman–Monteith formulation is commonly used to calculate the stomatal regulation of water flux (Monteith, 1966; Campbell and Norman, 1998). The resistance to flow regulated by the

stomata, R_{stomata} , is primarily a function of vapour pressure deficit (VPD), CO_2 concentration, plant species, and other factors. We note that this and the xylem resistance are the only variable resistors along the plant water transport pathway (e.g. the only resistor explicitly controlled by plant physiology). The atmospheric water potential, $\Psi_{\text{atm}}(\rho, e, T)$, is a function of water vapour density, water vapour pressure, and temperature. The advection and concentration of water can lead to high relative humidity and subsequent low flow of water from the plant to the atmosphere. The atmospheric water potential is calculated as $\Psi_{\text{atm}} = RT \ln(e/e^0)$ where R is the gas constant,

$8.31 \text{ J K}^{-1} \text{ mol}^{-1}$; T is the air temperature in Kelvin; e is the water vapour pressure; e^0 is the saturation water vapour pressure at temperature T ; e/e^0 is the fractional relative humidity; and the resulting value is in Pa. The resistance of flow at the plant canopy scale, R_{can} , is the sum of aerodynamic resistance to momentum transfer and the stomatal resistance.

Our current ability to quantify each process varies. Some processes such as the water potential difference required for moving water up a certain height of tree [$(\psi_{\text{xylem}}(g))$] are well understood and can be readily quantified. For example, Miller *et al.* (2010) modified Darcy's law and calculated ΔP_x —the maximum theoretical change in potential associated with overcoming gravity and the frictional resistance of the stem in order to reach a leaf at a given height above the ground as:

$$\Delta P_x = \rho_w z \left(\frac{q}{K_s} + g 10^{-6} \right) \quad (1)$$

where ρ_w is the density of water, 999 kg m^{-3} ; z is the length of the stem segment from the measurement point to the leaf height, in m; q_{max} is the maximum rate of sap ascent in the xylem measured by the sap flow sensors, in m s^{-1} ; K_s is the hydraulic conductivity of the stem, in $\text{kg s}^{-1} \text{ m}^{-1} \text{ MPa}^{-1}$; g is the gravitational acceleration constant, 9.81 m s^{-2} ; and 10^{-6} converts from Pa to MPa. However, other fundamental processes such as landscape scale partition of evaporation and transpiration (e.g. the relative contributions; Wang *et al.*, 2010) are less well understood, even with many theoretical values.

Similar to the plant resistor, for soil resistor (Figure 2(b)), all water flow is driven by potential gradients between the soil and atmosphere. $\Psi_{\text{soil}}(\theta)$ is a function of volumetric water content ($\text{m}^3 \text{ m}^{-3}$). $\Psi_{\text{atm}}(\rho, e, T)$, the atmospheric water potential, is a function of water vapour density, water vapour pressure, and temperature. R_{evap} , the resistance to flow from evaporation, includes resistance to water loss from interception by the canopy, litter, and also resistance to water loss from surface soil. Such resistance is primarily a function of VPD, temperature and soil properties including water content, temperature and diffusivity, etc. $I_{\text{rain}}(\rho, P, T)$ is current source of water from rainfall and is a function of water vapour density, pressure, and temperature in the atmosphere. Rainfall could be related to larger scale phenomena such as teleconnections (ENSO, DMI, etc.), inter-tropical convergence zone, and/or topography. Rainfall is often represented as a stochastic variable with some underlying statistical process (Rodriguez-Iturbe and Porporato, 2004; Laio *et al.*, 2006; Katul *et al.*, 2007). Rainfall here is assumed to be a steady-state variable (e.g. mean monthly, seasonal, or annual) to meet the circuit analogy requirement. For the current framework, the rainfall inputs and soil moisture are time-averaged (e.g. monthly and annual). The rainfall inputs may need to be modified further for pulse-driven ecosystems, those with growing seasons out-of-sync with precipitation and those with deep convection processes. The transient nature of soil

moisture may also need to be taken into account, which is critical in 'flashy (pulse-driven)' semi-arid ecosystems (Vereecken *et al.*, 2008; Wang *et al.*, 2009).

Plot/hillslope level

Building upon the plant and soil level information (Figure 2(a) and (b)), we incorporate the Thévenin equivalents from the plant and soil level into a larger scale—the plot or hillslope level (Figure 2(c)). This is the scale at which ecosystem flux measurements are made, typically using the eddy-covariance technique. The linkage between plant–soil and hillslope scales using the Thévenin equivalents provides potential opportunity to correlate ecosystem water flux and variations in plant functional types at smaller scale. As shown in Figure 2(c) for hillslope scale, water accumulates on the hillslopes and flows into the stream channel through various connections at different fluxes depending on the resistances. Surface roughness and vegetation patchiness result in numerous surface flowpaths (Ludwig *et al.*, 2002). Water that infiltrates into the soil leaves the hillslope at different times and depths, depending on the soil type and erosional processes (Lohse and Dietrich, 2005). In addition, soil macropores may exhibit threshold behaviour with increasing soil moisture and can potentially create short circuits in the system leading to large and rapid fluxes of water (Leonard and Rajot, 2001; Weiler and Naef, 2003). In the diagram, $\Psi_{\text{atm}}(\rho, R, T)$ is the atmospheric potential at the plant boundary layer. ψ_{atm} is a function of density, pressure, and temperature. R_{plant} (dashed box) and R_{evap} (dashed box) are the Thévenin equivalents from smaller scale. The plant equivalent could include a number of different plant resistors in parallel such as different plant resistances by C_3 , C_4 , or Crassulacean acid metabolism plants, different functional groups, grasses, trees, succulents, or a breakdown by species within functional groups. The soil water potential, $\Psi_{\text{soil}}(z, \theta)$, is a function of volumetric water content and gravitational potential (such as the elevation difference between the top of the hillslope and the stream channel). $R_{\text{overland_flow}}$ is the resistance to overland surface flow and is a function of surface roughness and topography. Resistance calculations may be related to roughness coefficients quantified through the Manning's equation for open channel flow. R_{unsat} is the resistance of flow due to the shallow unsaturated subsurface zone and is a function of water content, soil properties, and connectivity of the hillslope. R_{satzone} is the resistance of flow from the saturated subsurface and is a function of soil and rock properties and equal to the inverse of saturated hydraulic conductivity. The stream channel water potential, $\Psi_{\text{stream}}(z, vel)$, is a function of the elevation gradient and velocity of the stream.

Watershed level

As shown in Figure 2(d), $\Psi_{\text{atm}}(\rho, R, T)$, the atmospheric potential, is a function of density, pressure, and temperature at the plant boundary layer. $R_{\text{hillslope}}$ (dashed boxes) is the Thévenin equivalent found from the hillslope level using Thévenin's theory. These Thévenin

equivalents could include a number of different stream resistors in a branching series network. The stream channel water potential, $\Psi_{\text{stream}}(z, vel)$, is a function of the elevation and velocity of the stream. The channel resistance, R_{channel} , is the resistance of flow due to channel characteristics, such as length, travel time, and could be related to Bernoulli equations by linking flow speed and pressure. These stream channels refer to the streams not included in the hillslope scale. We could include a feedback to the atmosphere from transmission losses if desired. The watershed potential, $\Psi_{\text{watershed}}(z, vel)$, is a function of elevation and velocity. Continuing in this manner, the extensions to regional or continental scales which are represented by a series of connected watersheds are possible.

The watershed level incorporates the models from several hillslopes and multiple order streams, each with its own characteristics (Figure 2(d)). This helps account for spatial heterogeneity in landscape features that affect water movement. The accuracy of incorporating the river networks and hillslope vegetation distribution into the electrical analogy at watershed scale could be improved by better understanding of the organizational rules. For example, the spatial structure of channel networks displays power law behaviour indicating a dynamic self-organizing of the network (Rinaldo *et al.*, 1998). In addition, the structure of basin vegetation types (Caylor *et al.*, 2005) and species distribution patterns (Franz *et al.*, 2010) have been shown to organize in dryland ecosystems based on a resource trade-off hypothesis (Caylor *et al.*, 2009). Combining the principle of resource trade-offs with simple water balance models (such as the one presented above) may provide a tractable mathematical framework for understanding and explaining the emergent properties of dryland ecosystems across different scales affected by both 'eco' and 'hydro' processes.

To illustrate the applicability of using the Thévenin's theorem to explore across-scale interactions, we solve the electrical analogies at each level and apply it to a very simplified scenario: the effect of shrub encroachment on the hillslope scale water budget. In this case, we assume shrub encroachment will have two major effects: reduced evaporation (increase in R_{evap}) and more water uptake by trees (decrease in R_{plant}). We show that the changes at plant and soil scale will reduce the hillslope scale water flow (Figure 3). This is of course a rather oversimplified scenario, but it shows that with improved parameterization of the current, voltage source, and resistors, we could potentially quantify the across-scale water dynamics and interactions using the Thévenin's theorem.

Case II—carbon cycling in cells, leaves, and plants. Plants assimilate carbon dioxide through a series of interconnected biochemical and biophysical pathways that operate at sub-cellular to organismal scales but are the basis of large-scale processes, such as agricultural productivity and biosphere carbon flux. The assimilation models used to analyse and make predictions about

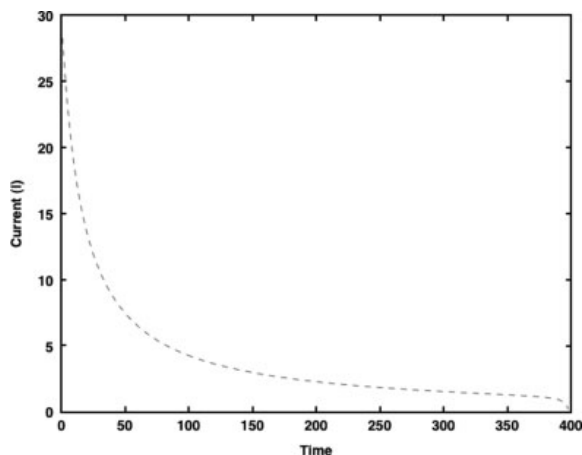


Figure 3. Response of water flow (current) to shrub encroachment at hillslope scale. In this simplified scenario, we assume shrub encroachment will have two major effects: reduced evaporation (increase in R_{evap}) and more water uptake by trees (decrease in R_{plant}) at individual plant and soil scale.

these processes generally rely on empirical relationships based on coarse spatial averages of vegetation parameters (Monteith, 1977; Collatz *et al.*, 1991) that do not account for small-scale interactions and heterogeneities.

In this section, the electrical circuit analogy is extended to carbon flow through ecosystems leading to a mechanistic model of plant carbon assimilation that can be scaled using the Thévenin's theorem. The movement of carbon occurs along concentration differences (voltage differences) and through the activity of carbon-fixing enzymes and active transport in plants (voltage sources). The connectivity of these pathways is determined by the plant attributes and the availability of light, water, and nutrients (resistances). Carbon flow (current) is equal to photosynthesis rate at the cell to leaf scale and net primary productivity (NPP) at the ecosystem scale. The following analogies are used (Table I):

- Voltage (V) is the concentration difference of carbon compounds in units of concentration (mol/m^3).
- Current (I) is carbon flux density ($\text{mol}/\text{m}^2/\text{s}$).
- Resistance (R) is the impedance to carbon flow of a link in the system (s/m) such that $I = V/R$.

We present electrical circuit analogies for a C_3 and a C_4 plants at the cell, leaf, and plant scale, showing where properties of the circuit can be connected to physiological measurements. By solving the circuits, we are able to analyse how disruptions to the connectivity of the system imposed by light and water limitation will differentially affect C_3 and C_4 plants. We use the Thévenin's theorem to upscale the circuits and infer how NPP is related to the proportion of C_3 and C_4 plants in a landscape under different water and light conditions.

Cell scale

The conversion of CO_2 to organic compounds is the result of the Calvin cycle, a series of reactions occurring in the

chloroplasts of photosynthetic cells. Carbon fixation is an energetically unfavourable process and requires inputs of energy from the light reactions of photosynthesis as well as catalysis by the enzyme RuBisCo (Calvin, 1959). RuBisCo can also catalyse a reaction with oxygen and initiate the photorespiratory cycle, which consumes energy but does not fix carbon (Ogren, 1984). The Calvin cycle is the same in C_3 and C_4 plants. C_4 plants differ in that they have a mechanism for preventing photorespiration, though it has an energetic cost (Ehleringer and Monson, 1993).

Figure 4(a) shows the electrical analogies for the photosynthetic pathways and cells of C_3 and C_4 plants. The CO_2 is introduced to the carbon fixation pathway, which is the same in C_3 and C_4 plants, at point A where RuBisCo catalyses its addition to the five-carbon compound ribulose 1,5-bisphosphate (RuBP), initiating the series of reactions. The availability of energy from the light reactions as adenosine triphosphate (ATP) and nicotinamide adenine dinucleotide phosphate (NADPH) is represented as resistances, which go to infinity in the absence of light. In the C_3 plant, RuBP may also be converted into a three-carbon intermediary compound without the incorporation of CO_2 . ATP is required for the regeneration of RuBP. Expressions for the RuBP carboxylation and oxygenation rates, given by $V_{S_{RuBisCo}}/R_{CO_2}$ and $V_{S_{RuBisCo}}/R_{O_2}$, were developed by Farquhar (1979). The necessary rate parameters have been determined *in vitro* using isotopic fractionation methods for a number of plant species (Tcherkez *et al.*, 2006 and references therein).

The Thévenin equivalents of the photosynthetic pathways can be used as components of circuit analogies for photosynthetic cells. In the C_3 cell, CO_2 reaches the carbon fixation system by diffusion through the cell and chloroplast membranes. The resistances associated with diffusion of CO_2 within the cells and across cell and organelle membranes are equal to the inverses of the diffusion coefficients that have been determined experimentally (Evans and Caemmerer, 1996; Gorton *et al.*, 2003) multiplied by the diffusion path length. The C_4 circuit encompasses two cells, with a strong diffusion barrier between them (Ludwig *et al.*, 1998). The first is a mesophyll cell where CO_2 binds with phosphoenolpyruvate (PEP) to form a four-carbon organic compound in a reaction catalysed by the enzyme PEP carboxylase that requires ATP. The compound is exported to a bundle sheath cell where it is converted back into PEP and CO_2 that can be assimilated. The carbon compound produced by the photosynthetic system is respired by the cell, stored as starch, or exported from the cell.

The mechanisms of light and nutrient limitation of photosynthesis operate at the cell scale as shortages of energy from the light reactions and nutrient-rich compounds such as RuBisCo reduce carbon fixation rates. These limitations can be imposed on the photosynthetic pathways in the model and the change on carbon flux through the photosynthetic cell observed. We simulated the effect of light

limitation on the C_3 and C_4 photosynthetic cells by solving the circuits for a range of ATP and NADPH resistance values (Figure 5(a)). At low resistances (high light availability), the inefficiency associated with photorespiration leads to lower carbon fluxes in the C_3 photosynthetic cell, but as energy from the light reactions becomes scarce, the energetic requirements of C_4 photosynthesis is limiting.

Leaf scale

CO_2 reaches the photosynthetic cells by diffusing through stomata on the leaf surface, the intercellular airspaces, and the cell membranes. Circuit analogies are widely used in describing the diffusion of CO_2 and water vapour into and out of leaves (Monteith, 1977), with the ease of flow through components of the system generally expressed as resistances (or conductances, the inverse). We coupled the established resistance model to the Thévenin equivalents of the photosynthetic cells. Active transport of photosynthate into the phloem for translocation to other parts of the plant also occurs in the leaves, and that is modelled here. Leaves provide the connection between CO_2 in the atmosphere and carbon in plant biomass, which is interrupted when plants close their stomata to avoid water stress.

Figure 4(b) shows the electrical analogy for a leaf with C_3 or C_4 photosynthetic cells. CO_2 must diffuse through the boundary layer, stomata, and intercellular airspace in series. Stomatal resistance is the largest barrier to CO_2 diffusion between the atmosphere and fixation in the chloroplasts (Taiz and Zeiger, 2006). The resistances in the model can be related to measured resistance values (expressed in s/m) or empirical estimates of stomatal resistance. The photosynthetic cells in the model are connected to the intercellular airspace in parallel. The cells do not need to be identical, so it is possible to account for heterogeneity in cell attributes such as RuBisCo abundance and light availability.

Leaves are assumed to be photosynthate sources. The carbon compounds produced by the photosynthetic cells are actively transported into the companion cells of the phloem sieve tubes. Phloem loading concentrates photosynthate in the phloem sap, and the voltage source associated with this process should reproduce measured concentration photosynthate in phloem sap (Doering-Saad *et al.*, 2002).

Diffusion of CO_2 into leaves via the stomata is inevitably accompanied by the diffusion of water vapour out of the leaf. When water availability is low, plants will increase stomatal resistance to avoid losing water. The effect of water stress on leaf photosynthesis rates can be investigated by solving for the Thévenin equivalent current of the leaf circuit analogy for different stomatal resistance values (Figure 5(b)). Increasing stomatal resistance results in a decrease in intercellular CO_2 concentrations. As the abundance of CO_2 decreases relative to the abundance of oxygen, photorespiration rates increase and the photosynthesis rate of the C_3 plant decreases more quickly than that of the C_4 plant (Berry and Downton, 1982).

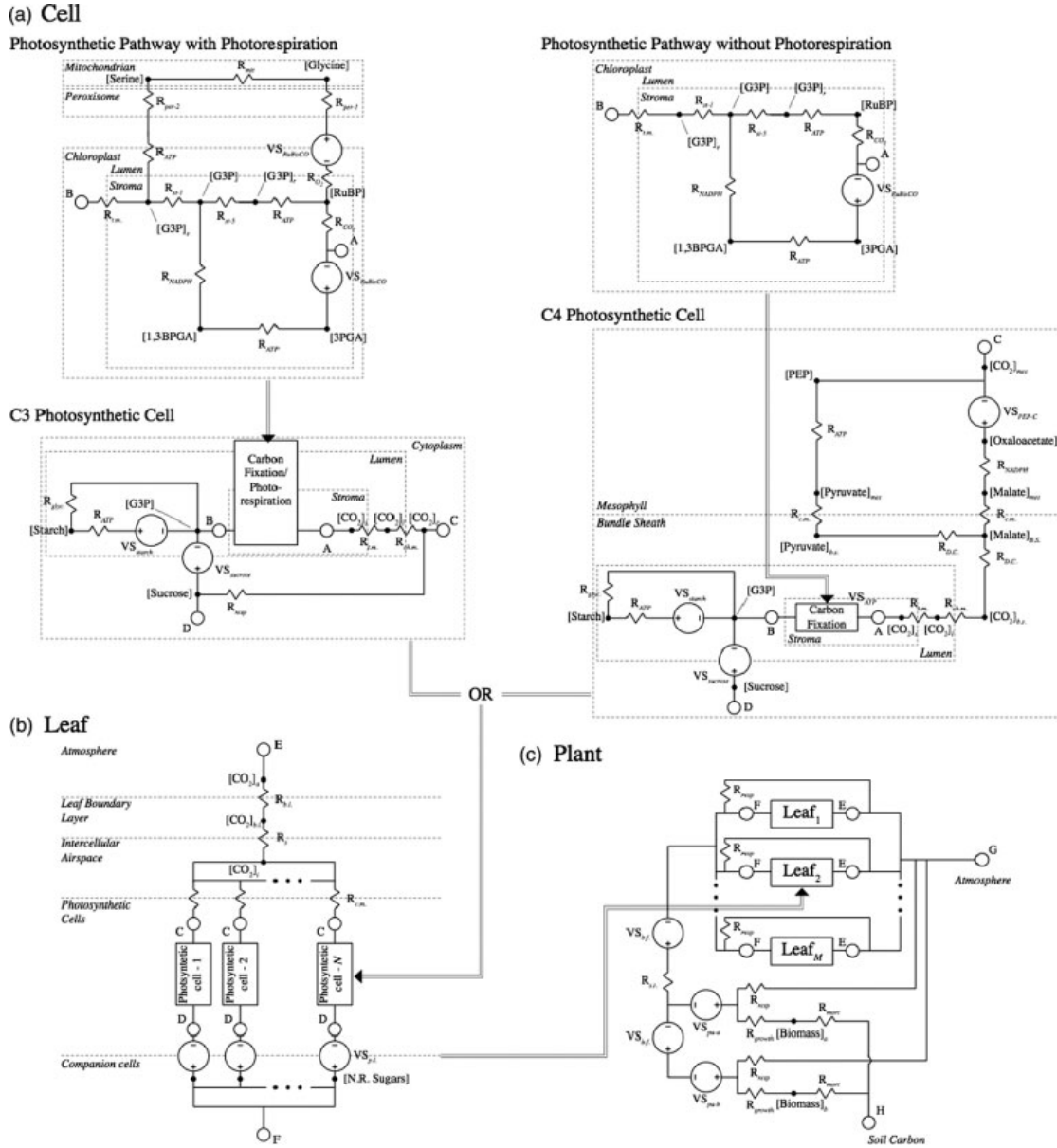


Figure 4. Diagram of electric circuit analogy for plant carbon assimilation. In this diagram, there are nodes, voltage sources, and resistances. For nodes, (RuBP) is ribulose 1,5-bisphosphate, (3PGA) is 3-phosphoglycerate, (1,3BPGA) is 1,3-bisphosphoglycerate, (G3P) is glyceraldehyde-3-phosphate, $(G3P)_e$ is exported glyceraldehyde-3-phosphate, $(G3P)_r$ is glyceraldehyde-3-phosphate for regeneration of RuBP, $(CO_2)_c$, $(CO_2)_l$, and $(CO_2)_s$ are carbon dioxide in the cytoplasm, lumen, and stroma, (Glycine) and (Serine) are glycine and serine, intermediates in the photorespiratory pathway, (1,3BPGA) is 1,3-bisphosphoglycerate, (Starch) is carbon stored as starch in the chloroplast, (Sucrose) is carbon available as sucrose for cellular respiration and export to the phloem, $(CO_2)_a$, $(CO_2)_{b,l}$, and $(CO_2)_i$ are carbon dioxide in the atmosphere, leaf boundary layer, and intercellular space, (N.R. Sugars) is non-reducing sugars in the phloem companion cells, $(Biomass)_a$ is non-leaf aboveground biomass, $(Biomass)_b$ is belowground biomass. For voltage sources, $VS_{RuBisCO}$ represents the enzyme ribulose 1,5-bisphosphate carboxylase-oxygenase (RuBisCO) catalyzing the reaction between CO_2 (introduced at point A) or oxygen with RuBP, VS_{starch} is the production of starch in the chloroplast, catalysed by ADP-glucose pyrophosphorylase, $VS_{sucrose}$ is the production of sucrose for cellular respiration and export to the phloem, catalysed by sucrose phosphate synthetase, $VS_{p,l}$ is the phloem loading, the active transport of sucrose from photosynthetic cells to phloem companion cells, $VS_{b,f}$ is the transport of sugar by bulk flow in the phloem, VS_{pu-a} and VS_{pu-b} are phloem unloading into aboveground and belowground biomass. For resistances, R_{ATP} and R_{NAPH} are the resistances associated with the production of ATP and NADPH by the light reactions. These go to infinity in the absence of light, R_{st-1} and R_{st-5} are resistances imposing a 5:1 stoichiometric ratio between carbon exported from the stroma and carbon used in the regeneration of RuBP, $R_{t,m}$ is the resistance associated with diffusion across the thylakoid membrane, $R_{ch,m}$ is the resistance associated with diffusion across the chloroplast membrane, R_{ATP} and R_{NAPH} are the resistances associated with the production of ATP and NADPH by respiration, R_{CO_2} and R_{O_2} are the resistances associated with the bonding of RuBisCo with carbon dioxide and oxygen, R_{mit} and R_{per} are the resistances associated with diffusion through the mitochondria and peroxisomes, R_{glyc} is the resistance regulating the rate of glycolysis of starch to G3P, R_{resp} is the resistance regulating the rate of conversion of sucrose to carbon dioxide by cellular respiration, $R_{b,l}$ is the resistance associated with diffusion of carbon dioxide through the leaf boundary layer, R_s is the resistance associated with diffusion of carbon dioxide through the stomata, $R_{c,m}$ is the resistance associated with diffusion of carbon dioxide across the cell membrane, $R_{t,t}$ is the resistance associated with movement through the phloem sieve elements, R_{growth} is the resistance regulating the rate of conversion of sucrose into plant tissues, R_{mort} is the resistance regulating the rate of conversion of plant tissue into detritus through mortality.

Plant scale

Carbon moves through the plant from sources in the leaves to sinks in aboveground and belowground non-photosynthetic tissues. We represent leaves in the model by their Thévenin equivalents, and heterogeneity related to canopy position and leaf size can be incorporated. Sugars are transported from the leaves via bulk flow in the phloem and unloaded at sink tissues. The mechanisms behind these processes are still a topic of debate and active research. The model framework used here is sufficiently general that adjusting the parameter values could accommodate both active and passive models of phloem transport. For the circuit analogy to work, we must assume that the sources and sinks are in steady state. To analyse NPP at the ecosystem scale, multiple plants with different characteristics can be put into a circuit in series.

Figure 4(c) shows the electrical circuit analogy for a plant with multiple leaves. The leaves with the lowest numbers are farthest from the centre of the tree. A more complex branching structure could be introduced by changing the pathways along which the F terminals of the leaves are connected. According to the pressure-flow model of phloem translocation (Munch, 1930), phloem loading at the source tissues generates a negative solute potential, increasing the turgor pressure of the cells, and unloading at the sink tissues generates a positive solute potential, decreasing turgor pressure. Water moves from high pressure to low pressure with some resistance from the membranes separating sieve tube elements and moving sugars by advection. The voltage sources associated with bulk flow and resistance associated with sieve tubes should generate a current that agrees with measured phloem mass transfer rates (Peuke *et al.*, 2001).

The circuits for multiple plants with different attributes can be connected in series to simulate an ecosystem, with current through the parallel circuit analogous to NPP. We solved circuits representing ecosystems with combinations of C_3 and C_4 plants under water-limited (high stomatal resistance) and light-limited (low ATP and NADPH availability) conditions (Figure 5(c)). Our analysis shows, using the electrical circuit analogy scaled with the Thévenin's theorem, how decreases in the connectivity of small-scale carbon assimilation pathways translate into changes in ecosystem scale carbon dynamics.

Case III—nitrogen transport in plant, plant–soil and hillslope level. In this case application, we will illustrate the nitrogen transport across different scales: plant, plant–soil, and hillslope levels. Similar to former sections, we construct a hierarchy of electric analogies for each level based on current understanding of nitrogen transport. We will solve the diagrams at the first two levels (plant and plant–soil) to indicate cross-scale interactions. In all the nitrogen transport diagrams, the following analogies are used (Table I):

- Voltage (V) is the concentration difference of nitrogen compounds in units of concentration (mol/m^3).

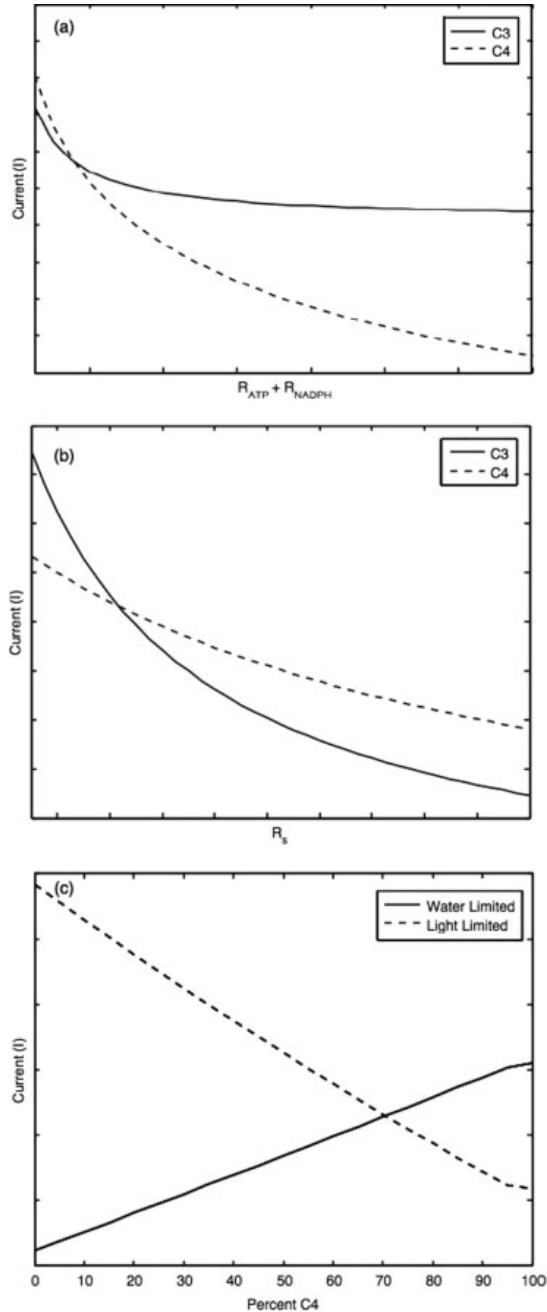


Figure 5. (a) Response of carbon flow (current) through C_3 and C_4 photosynthetic cells over a range of values for the resistance associated with energy inputs from the light reactions of photosynthesis. High resistance values are associated with light limitation. (b) Carbon flow (current) through C_3 and C_4 leaves over a range of values for stomatal resistance. High resistance values are associated with water limitation. (c) Carbon flow (current) through varying assemblages of plant circuits connected in parallel. Plants in the water-limited system have high stomatal resistance and low resistances associated with ATP and NADPH availability. The light-limited system has low stomatal resistance and high resistances associated with ATP and NADPH availability.

- Current (I) is nitrogen flux density ($\text{mol}/\text{m}^2/\text{s}$).
- Resistance (R) is the impedance to nitrogen flow of a link in the system (s/m).

This exercise aims to demonstrate another example of using the Thévenin's theorem to upscale connectivity interaction to different scales, as long as the interactions are well represented in the electrical analogy circuits.

Plant scale

Nitrogen plays a critical role in plant growth, as it is required for the synthesis of amino acids, proteins, and DNA. Nitrogen transport within plants is ultimately driven by the demand from leaf photosynthesis enzymes and compounds, e.g. RuBisCo and chlorophyll. About 5–30% of RuBisCo (depends on plant functional types) and 6% of chlorophyll are composed of nitrogen, by mass. The form of nitrogen that is transported from the assimilatory root to the shoot has been found to vary widely among higher plants (McClure and Israel, 1979). Nitrate, amino acids, amides, and ureides all have been reported as principal forms of nitrogen in the xylem sap of various plants (Bollard, 1957; McClure and Israel, 1979; Kato, 1981). Nitrogen can also be transported in the phloem, but it is normally in the form of amino acids and amides. Nitrate (NO_3^-) can be incorporated into organic compounds in both root and leaf tissue, whereas ammonia (NH_4^+) is only synthesized into amino acids in the root tissues near the site of uptake to avoid toxic accumulation (Engels and Marschner, 1995). As a result, ammonium is rarely seen in xylem sap. The plant nitrogen transport process within xylem is simplified by Figure 6(a). In this diagram, V_{xylem} and V_{leaf} are nitrogen pools in xylem and leaves. $VS_{\text{plant_demand}}$ is the voltage source associated with plant nitrogen demand at leaves, which is the driven force of nitrogen transport. R_{NH_3} is the resistance associated with ammonium fraction transport in xylems, R_{NO_3} is the resistance associated with nitrate transport in xylem, and $R_{\text{organic nitrogen}}$ is the resistance associated with organic nitrogen (e.g. ureide and glutamine) transport in xylem. All the voltage and resistance terms are species-specific or even developmental stage-specific, but they are quantifiable, and as long as there are parameter inputs, they could be simplified into a Thévenin equivalent.

Plant–soil scale

Nitrogen transport within plants could be simplified as a Thévenin equivalent (R_{plant}) and placed into plant–soil scale. In this scale, plants take up nitrogen (e.g. NH_4 and NO_3 , dissolved organic nitrogen) from soils; these nitrogen compounds are assimilated inside roots/shoots and transported to various organs for assimilation. As organic nitrogen uptake usually only occurs in extremely nitrogen-limited situations (Chapin *et al.*, 2002), the plant nitrogen uptake in this article focuses on only inorganic nitrogen (mainly ammonium and nitrate) uptake. Either NH_4^+ or NO_3^- can dominate the inorganic N pool of an ecosystem; for example, in most mature undisturbed forests, the soil inorganic N pools are dominated by NH_4^+ (Kronzucker *et al.*, 1997). In well-aerated agricultural soils or frequently disturbed sites, NO_3^- is the principal inorganic N source (Brady and Weil, 1999). The

plant nitrogen transport process within plant–soil scale is simplified by Figure 6(b). As it shows, the $R_{\text{NO}_3 \text{ uptake}}$ is the resistance associated with nitrate uptake in roots, which is a function of soil moisture in many model representations (Porporato *et al.*, 2003; Wang *et al.*, 2009). The $VS_{\text{ammonium uptake}}$ is the voltage source associated with plant ammonium uptake. Plant ammonium uptake is a voltage source because ammonium is a cation and its uptake depends on active transport mechanisms, e.g. again energy and concentration gradient. The assimilation of NH_4^+ is more energetically efficient when compared to NO_3^- , because NH_4^+ can be directly incorporated into glutamate via an NH_4^+ assimilation pathway. Nitrate, on the other hand, must first be modified via a reduction pathway before assimilation (Engels and Marschner, 1995). In addition to ammonium and nitrate uptake from soil, biological nitrogen fixation converts atmosphere nitrogen ($V_{\text{atmosphere}}$) into ammonia, providing a source for plant nitrogen. The $VS_{\text{atmosphere nitrogen}}$ is the voltage source associated with nitrogen fixation as nitrogen fixation process is strongly against energy gradient. The plant nitrogen (V_{leaf}), including both leaf and root nitrogen, will go to soil through litterfall and root decomposition and eventually go into soil organic nitrogen pool (V_{SOM}). Soil organic nitrogen will be mineralized into ammonium pool (V_{ammonium}) and nitrated into nitrate pool (V_{nitrate}). The R_{min} and $R_{\text{nitrification}}$ are resistances associated with mineralization and nitrification process. Soil nitrate pool (V_{nitrate}) is also connected to atmosphere nitrogen pool ($V_{\text{atmosphere}}$) through denitrification process ($R_{\text{denitrification}}$), which is controlled by soil water content, nitrate concentration, microbe species, and abundance.

Hillslope scale

Building upon the plant–soil level model, we incorporate multiple Thévenin equivalents (e.g. multiple plant–soil interactive systems) into a larger scale—the hillslope level. Hillslope scale nitrogen transport is simplified as in Figure 6(c). At the hillslope level, besides the similar processes at plant–soil scale, the nitrogen transport includes atmospheric nitrogen deposition ($R_{\text{nitrogen deposition}}$) and the subsequent nitrogen loss including surface runoff ($R_{\text{surface runoff}}$) and groundwater leaching ($R_{\text{groundwater leaching}}$). This is no doubt a simplified nitrogen transport representation at the hillslope level, but it captures the essential components of nitrogen transformation processes. Most importantly, this representation incorporates the Thévenin equivalents of plant–soil level and could be simplified into Thévenin equivalent, and used for larger scales (e.g. watershed scale).

As mentioned in the previous section, both inorganic nitrogen (e.g. nitrate) and organic nitrogen (e.g. amino acids, amides, and ureides) can serve as principal forms of nitrogen in the xylem sap. We solve circuits representing individual plant scale and plant–soil scale to indicate the cross-scale interactions (Figure 7). Our analysis shows, if we hold everything else constant, that higher percentage of nitrogen flow in inorganic form at individual level

CHARACTERIZE CONNECTIVITY ACROSS SCALES

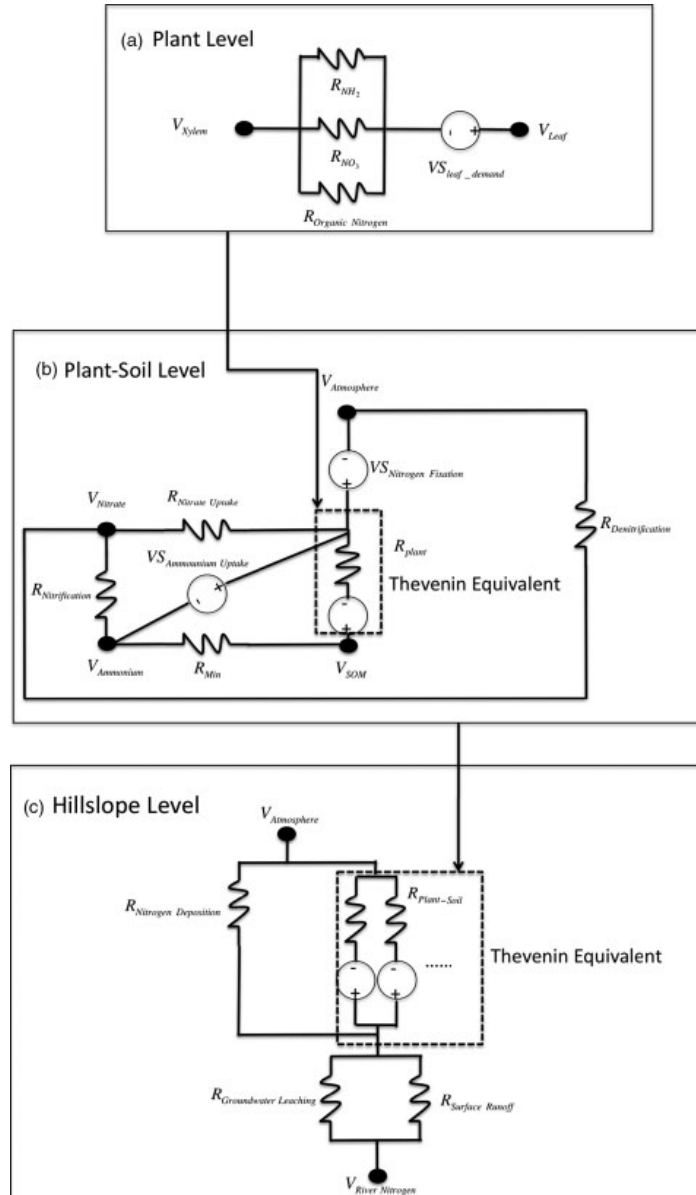


Figure 6. Diagram of electric circuit analogy for nitrogen transport at plant level (a), plant-soil level (b), and hillslope level (c). For plant level, V_{xylem} and V_{leaf} are nitrogen pool in xylem and leaves, R_{NH_3} is the resistance associated with ammonium fraction transport in xylems, R_{NO_3} is the resistance associated with nitrate transport in xylem and $R_{organic\ nitrogen}$ is the resistance associated with organic nitrogen transport in xylem. VS_{plant_demand} is the voltage source associated with plant nitrogen demand at leaves. For plant-soil level, $V_{ammonium}$, $V_{nitrate}$, V_{SOM} , and $V_{atmosphere}$ are nitrogen pools in ammonium, nitrate, soil organic matter, and atmospheric components, $R_{nitrate\ uptake}$ is the resistance associated with nitrate uptake in roots, $VS_{ammonium\ uptake}$ is the voltage source associated with plant ammonium uptake, R_{min} , $R_{denitrification}$, and $R_{nitrification}$ are resistances associated with mineralization, denitrification, and nitrification processes, $VS_{nitrogen\ fixation}$ is the voltage source associated with nitrogen fixation, R_{plant} (dashed box) is the Thévenin equivalent from plant scale. For hillslope level, $V_{atmosphere}$ is nitrogen pool in atmospheric component, $R_{nitrogen\ deposition}$, $R_{surface\ runoff}$, and $R_{groundwater\ leaching}$ are the resistances associated with atmospheric nitrogen deposition, surface runoff, and groundwater leaching. $R_{plant-soil}$ (dashed box) is the Thévenin equivalent from the plant-soil scale.

leads to higher overall nitrogen flow at plant-soil level (Figure 7).

SUMMARY AND FUTURE DIRECTIONS

We demonstrate the possibility of using Thévenin's theorem connecting three different ecosystem processes

across scales: water transport, carbon transport, and nitrogen transport. Though preliminary, these examples show that the Thévenin's theorem could be successfully used for upscaling connectivity for various ecohydrological and biogeochemical processes. The Thévenin's theorem provides the ability to represent complex environmental processes with a simplified circuit and allows for straightforward combinations of the Thévenin equivalents that

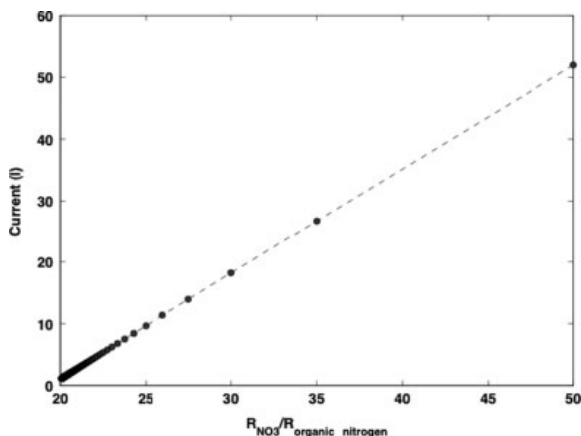


Figure 7. Response of nitrogen flow (current) over a range of resistance values at plant–soil level, which are associated with NO_3 and organic nitrogen transport at individual plant scale.

are developed at one scale (e.g. a Thévenin equivalent circuit for a single plant) to simulate processes at a larger scale (e.g. combination of equivalent plant circuits forming a circuit representing a hillslope). As the Thévenin equivalent behaves identically to that of the original circuit, any mechanistic representation is maintained when moving to larger scales. The influence and connectivity of elements at the micro-level on resultant processes at the macro-level may then be investigated.

The limitations of using Thévenin's theorem for upscaling connectivity lie in: (1) the ability to accurately represent ecosystem processes using electrical analogies and (2) the applicability of the Thévenin's theorem only to linear circuits. Nonlinearity is a common phenomenon in biophysical processes, e.g. the stomata response to variations of soil moisture may not be linear. The first limitation may be alleviated as our understanding of different ecosystem processes improves and the second limitation could be potentially bypassed by breaking down nonlinear circuits into smaller linear ones or by linearizing over finite ranges of behaviour. In addition, for small-scale complex processes where underlying mechanisms are not fully understood, the Thévenin equivalents may still be developed using a technique similar to that of the laboratory procedure for measuring voltages with a variable resistor (cf. section of the Thévenin's theorem concept and principles).

Future work will include refining the electrical analogue of different ecosystem processes and better parameterization of the voltage, resistor, and current sources. For example, the resistor terms at plant and soil scale are generally well quantified in many systems, but they are much less known for the hillslope and watershed scales. In addition, each process (e.g. water and nitrogen) is presented as a separated electrical analogy for simplicity. However, across water-limited arid and semi-arid environments, it has been long recognized that pulsed water events strongly impact the biogeochemical cycling of various elements (Austin *et al.*, 2004). For example, small rainfall events in drylands will promote 'hot moments'

of increased CO_2 (the birch effect) and NO_x production. In addition, the spatial heterogeneity of arid environments leads to 'hot spot' locations (e.g. under the tree canopies, or in riparian zones) where reaction rates are disproportionately high relative to the surrounding matrix (Schlesinger *et al.*, 1990; McClain *et al.*, 2003; Ravi *et al.*, 2009). As a further step for describing and understanding ecosystem processes, water, carbon, and nitrogen transport may need to be explicitly combined into one framework when the processes are intimately linked, e.g. photosynthesis from sub-cellular level to canopy scale.

ACKNOWLEDGMENTS

LW acknowledges the financial support from an NSF CAREER award to K. Caylor (EAR 847368). BB acknowledges support from the National Science Foundation (DEB-0416060). The clarity and strength of this article have been improved by the detailed comments from two anonymous reviewers.

REFERENCES

- Austin AT, Yahdjian L, Stark JM, Belnap J, Porporato A, Norton U, Ravetta DA, Schaeffer SM. 2004. Water pulses and biogeochemical cycles in arid and semiarid ecosystems. *Oecologia* **141**: 221–235.
- Berry J, Downton J. 1982. Environmental regulation of photosynthesis. In *Photosynthesis. Volume II. Development, Carbon Metabolism, and Productivity*, Govindjee (eds). Academic Press: New York; 263–343.
- Bollard E. 1957. Translocation of organic nitrogen in the xylem. *Australian Journal of Biological Sciences* **10**: 292–301.
- Boylestad R. 1982. In *Introductory Circuit Analysis*, Charles E (ed). Merrill Publishing Company: Upper Saddle River, NJ.
- Brady NC, Weil RR. 1999. *The Nature and Properties of Soil*. Prentice Hall: Upper Saddle River, NJ.
- Calvin M. 1959. Energy reception and transfer in photosynthesis. *Review of Modern Physics* **31**: 147–156.
- Campbell G. 2003. Modeling sensible and latent heat transport in crop and residue canopies. *Agronomy Journal* **95**: 1388–1392.
- Campbell G, Norman J. 1998. *An Introduction to Environmental Biophysics*. Springer: New York.
- Caylor KK, Manfreda S, Rodriguez-Iturbe I. 2005. On the coupled geomorphological and ecohydrological organization of river basins. *Advances in Water Resources* **28**: 69–86.
- Caylor KK, Scanlon TM, Rodriguez-Iturbe I. 2009. Ecohydrological optimization of pattern and processes in water-limited ecosystems: a trade-off-based hypothesis. *Water Resources Research* **45**: 15.
- Chapin F, Matson P, Mooney H. 2002. *Principles of Terrestrial Ecosystem Ecology*. Springer-Verlag: New York.
- Clapp R, Hornberger G. 1978. Empirical equations for some soil hydraulic properties. *Water Resource Research* **14**: 601–604.
- Collatz C, Ball J, Grievet C, Berry J. 1991. Physiological and environmental regulation of stomatal conductance, photosynthesis, and transpiration: a model that includes a laminar boundary layer. *Agricultural and Forest Meteorology* **54**: 107–136.
- Cosby B, Hornberger G, Clapp R, Ginn T. 1984. A statistical exploration of the relationships of soil moisture characteristics to the physical properties of soils. *Water Resource Research* **20**: 682–690.
- Dewar R. 2002. The Ball-Berry-Leuning and Tardieu-Davies stomatal models: synthesis and extension within a spatially aggregated picture of guard cell function. *Plant Cell and Environment* **25**: 1383–1398.
- Dingman S. 2008. *Physical Hydrology*. Waveland Press, Inc.
- Doering-Saad C, Newbry H, Bale J, Pritchard J. 2002. Use of aphid styletometry and RT-PCR for the detection of transporter mRNAs in sieve elements. *Journal of Experimental Botany* **53**: 631–637.
- Dorf R, Svoboda J. 2006. *Introduction to Electric Circuits*. John Wiley and Sons, Inc: Hoboken, NJ.
- Ehleringer J, Monson R. 1993. Evolutionary and ecological aspects of photosynthetic pathway variation. *Annual Review of Ecological Systems* **24**: 411–439.

- Engels C, Marschner H. 1995. Plant uptake and utilization of nitrogen. In *Nitrogen Fertilization in the Environment*. Bacon P (ed). Woodlotts and Wetlands Pty. Ltd: Sydney; 41–81.
- Evans J, Caemmerer Sv. 1996. Carbon dioxide diffusion inside leaves. *Plant Physiology* **110**: 339–346.
- Farquhar GD. 1979. Models describing the kinetics of ribulose biphosphate carboxylase–oxygenase. *Archives of Biochemistry and Biophysics* **2**: 456–468.
- Fitter A, Hay R. 1987. *Environmental Physiology of Plants*. Academic Press: San Diego, CA.
- Franz T, Caylor K, Nordbotten J, Rodriguez-Iturbe I, Celia M. 2010. An ecohydrological approach to predicting regional woody species distribution patterns in dryland ecosystems. *Advances in Water Resources* **33**: 215–230. DOI: 210.1016/j.advwatres.2009.10.12.1003.
- Gorton H, Herbert S, Vogelmann T. 2003. Photoacoustic analysis indicates that chloroplast movement does not alter liquid-phase CO₂ diffusion in leaves of *Alocasia brisbanensis*. *Plant Physiology* **132**: 1529–1539.
- Honert TH. 1948. Water transport in plants as a catenary process. *Discussions of the Faraday Society* **3**: 146–153.
- Jarvis P, Edwards W, Talbot H. 1981. Models of plant and crop water use. In *Mathematics and Plant Physiology*. Rose DA and Charles-Edwards DA (eds). Academic Press: London; 151–194.
- Jones H. 1992. *Plants and Microclimate*. Cambridge University Press: New York, NY.
- Kato T. 1981. Major nitrogen compounds transported in xylem vessels from roots to top in Citrus trees. *Physiologia Plantarum* **52**: 275–279.
- Katul G, Porporato A, Oren R. 2007. Stochastic dynamics of plant–water interactions. *Annual Review of Ecology Evolution and Systematics* **38**: 767–791.
- Kramer P, Boyer J. 1995. *Water Relations of Plants and Soils*. Academic Press: San Diego, CA.
- Kramer PJ. 1974. Fifty years of progress in water relations research. *Plant Physiology* **54**: 463–471.
- Kronzucker H, Siddiqi M, Glass A. 1997. Conifer root discrimination against soil nitrate and the ecology of forest succession. *Nature* **385**: 59–61.
- Laio F, D'Odorico P, Ridolfi L. 2006. An analytical model to relate the vertical root distribution to climate and soil properties. *Geophysical Research Letters* **33**: L18401. DOI: 18410.11029/12006GL027331.
- Leonard J, Rajot JL. 2001. Influence of termites on runoff and infiltration: quantification and analysis. *Geoderma* **104**: 17–40.
- Lohse KA, Dietrich WE. 2005. Contrasting effects of soil development on hydrological properties and flow paths. *Water Resources Research* **41**: 17.
- Ludwig JA, Eager RW, Bastin GN, Chewings VH, Liedloff AC. 2002. A leakiness index for assessing landscape function using remote sensing. *Landscape Ecology* **17**: 157–171.
- Ludwig M, Caemmerer Sv, Price G, Badger M, Furbank R. 1998. Expression of tobacco carbonic anhydrase in the C₄ dicot *Flaveria bidentis* leads to increased leakiness of the bundle sheath and a defective CO₂ concentrating mechanism. *Plant Physiology* **117**: 1071–1082.
- McClain ME, Boyer EW, Dent CL, Gergel SE, Grimm NB, Groffman PM, Hart SC, Harvey JW, Johnston CA, Mayorga E, McDowell WH, Pinay G. 2003. Biogeochemical hot spots and hot moments at the interface of terrestrial and aquatic ecosystems. *Ecosystems* **6**: 301–312.
- McClure PR, Israel DW. 1979. Transport of nitrogen in the xylem of soybean plants. *Plant Physiology* **64**: 411–416.
- Miller G, Chen X, Rubin Y, Ma S, Baldocchi D. 2010. Groundwater uptake by woody vegetation in a semi-arid oak savanna. *Water Resources Research* **46**: W10503. DOI: 10.1029/2009WR008902.
- Monteith J. 1966. Photosynthesis and transpiration of crops. *Experimental Agriculture* **2**: 1–14.
- Monteith J. 1977. Climate and the efficiency of crop production in Britain. *Philosophical Transactions of the Royal Society of London B* **281**: 277–294.
- Munch E. 1930. *Die Stoffbewegungen in der Pflanze*. Gustav Fischer: Jena, Germany.
- Ogren W. 1984. Photorespiration: pathways, regulation and modification. *Annual Review of Plant Physiology* **35**: 415–422.
- Peters D, Pielke SR, Bestelmeyer B, Allen C, Munson-McGee S, Havstad K. 2004. Cross-scale interactions, nonlinearities, and forecasting catastrophic events. *Proceedings National Academy of Sciences, USA* **101**: 15130–15135.
- Peters DPC, Bestelmeyer BT, Herrick JE, Fredrickson EL, Monger HC, Havstad KM. 2006. Disentangling complex landscapes: new insights into arid and semiarid system dynamics. *Bioscience* **56**: 491–502.
- Peuke A, Rokitta M, Zimmermann U, Schreiber L, Haase A. 2001. Simultaneous measurement of water flow velocity and solute transport in xylem and phloem of adult plants of *Ricinus communis* over a daily time course by nuclear magnetic resonance spectrometry. *Plant Cell and Environment* **24**: 491–503.
- Philip JR. 1966. Plant water relations: some physical aspects. *Annual Review of Plant Physiology* **17**: 245–268.
- Porporato A, D'Odorico P, Laio F, Rodriguez-Iturbe I. 2003. Soil moisture controls on the nitrogen cycle I: modeling scheme. *Advances in Water Resources* **26**: 45–58.
- Ravi S, D'Odorico P, Wang L, White CS, Okin GS, Macko SA, Collins SL. 2009. Post-fire resource redistribution in desert grasslands: a possible negative feedback on land degradation. *Ecosystems* **12**: 434–444.
- Rinaldo A, Rodriguez-Iturbe I, Rigon R. 1998. Channel networks. *Annual Review of Earth and Planetary Sciences* **26**: 289–327.
- Rodriguez-Iturbe I, Porporato A. 2004. *Ecohydrology of Water-Controlled Ecosystems*. Cambridge University Press: New York; 442.
- Schaap MG, Leij FJ, van Genuchten MT. 2001. ROSETTA: a computer program for estimating soil hydraulic parameters with hierarchical pedotransfer functions. *Journal of Hydrology* **251**: 163–176.
- Schlesinger WH, Reynolds JF, Cunningham GL, Huenneke LF, Jarrell WM, Virginia RA, Whitford WG. 1990. Biological feedbacks in global desertification. *Science* **247**: 1043–1048.
- Taiz L, Zeiger E. 2006. *Plant Physiology*. Sinauer: Sunderland, MA.
- Taylor P, Fahrig L, Henein K, Merriam G. 1993. Connectivity is a vital element of landscape structure. *Oikos* **68**: 571–573.
- Tcherkez G, Farquhar G, Andrews T. 2006. Despite slow catalysis and confused substrate specificity, all ribulose biphosphate carboxylases may be nearly perfectly optimized. *Proceedings of the National Academy of Sciences, USA* **103**: 7246–7251.
- Tischendorf L, Fahrig L. 2000. On the usage and measurement of landscape connectivity. *Oikos* **90**: 7–19.
- Tuzet A, Perrier A, Leuning R. 2003. A coupled model of stomatal conductance, photosynthesis and transpiration. *Plant Cell and Environment* **26**: 1097–1116.
- Tyree MT, Ewers FW. 1991. The hydraulic architecture of trees and other woody plants. *New Phytologist* **119**: 345–360.
- Vereecken H, Huisman JA, Bogaen H, Vanderborght J, Vrugt JA, Hopmans JW. 2008. On the value of soil moisture measurements in vadose zone hydrology: a review. *Water Resources Research* **44**: W00D06. doi:10.1029/2008WR006829.
- Wang L, Caylor KK, Villegas JC, Barron-Gafford GA, Breshears DD, Huxman TE. 2010. Evapotranspiration partitioning with woody plant cover: assessment of a stable isotope technique. *Geophysical Research Letters* **37**: L09401. DOI: 09410.01029/02010GL043228.
- Wang L, D'Odorico P, Manzoni S, Porporato A, Macko S. 2009. Carbon and nitrogen dynamics in southern African savannas: the effect of vegetation-induced patch-scale heterogeneities and large scale rainfall gradients. *Climatic Change* **94**: 63–76.
- Weiler M, Naef F. 2003. Simulating surface and subsurface initiation of macropore flow. *Journal of Hydrology* **273**: 139–154.
- Zhang H, Hou J. 2005. Maintaining sensing coverage and connectivity in large sensor networks. *Ad Hoc and Sensor Wireless Networks* **1**: 89–124.